❒ 696

Circuit Modelling of Bandpass/Channel Filter with Microstrip Implementation

Augustine O. Nwajana
School of Engineering, University of Greenwich, United Kingdom

Article Info	ABSTRACT
	This paper presents a step-by-step approach to the design of bandpass/channel filters. A 3-pole Chebyshev bandpass filter (BPF) with centre frequency of 2.6 GHz, fractional bandwidth of 3%, passband ripple of 0.04321 dB and return loss of 20 dB has been designed, implemented, and simulated. The designed filter implementation is based on the Rogers RT/Duroid 6010LM substrate with a 10.7 dielectric constant and 1.27 mm thickness. The BPF was also fabricated using the same substrate material used for the design simulation. The circuit model and microstrip layout results of the BPF are presented and show good agreement. The microstrip layout simulation results show that a less than 1.8 dB minimum insertion loss and a greater than 25 dB in-band return loss were achieved. The overall device size of the BPF is 18.0 mm by 10.7 mm, which is equivalent to $0.16\lambda g$ x $0.09\lambda g$, where λg is the guided wavelength of the 50 Ohm microstrip line at the filter centre frequency.

Corresponding Author:

Augustine O. Nwajana
School of Engineering,
University of Greenwich,
ME4 4TB, UK.
Email: a.nwajana@ieee.org

1. INTRODUCTION

A channel filter, also known as bandpass filter (BPF) passes frequencies within a single band and rejects all other frequencies outside the band [1]. This type of filter is widely used as the building block in the design of complex and multi-port circuits and systems. Some of the more complex devices that can be formed from BPFs include filtering antennas [2,3], multi-band filters [4–6], filtering power dividers [7,8], diplexers [9,10], etc. Figure 1 shows the response from a bandpass filter that passes all signal components between a lower frequency limit, f_L and an upper frequency limit, f_H, while attenuating and rejecting all other signal components that fall outside the f_L and f_H band. A bandpass filter can be formed by combining a lowpass filter with a highpass filter. Bandpass filters are widely used in radio frequency (RF) front end of cellular radio base station transceivers. Its main function in the transmitter is to limit the bandwidth of the output signal to the band assigned for the transmission. By this, the transmitter is prevented from interfering with other stations. In the receiver, a bandpass filter permits signals within a certain band of frequencies to be received and decoded, while stopping signals at undesirable frequencies from getting through.

Many authors have reported BPFs designed and implemented using various transmission line technologies including waveguides [11–13], microstrip [14–17] and substrate integrated waveguide [18–20]. The BPF presented in this paper is based on the microstrip technology. The filter relies on the microstrip hairpin resonator to achieve compact size. It is also of high selectivity and sharp roll-off. Some filter design characteristics such as selectivity, cost, size, sensitivity to environmental effects, power handling capacity, in-band and out-of-band performance metrics, are critical specifications in the development of RF and microwave communication front end devices. Filter developers are often required to make compromise between several conflicting requirements as it is rather difficult or even physically and/or electrically impossible to

simultaneously achieve all design criteria or specifications. For instance, achieving higher channel selectivity usually requires the use of more resonators, which will result in higher insertion loss along the transmission path since insertion loss is approximately proportional to the number of resonators used in the construction of a filter [1]. Hence, care must be taken when selecting design specifications to meet the most critical design targets.

Some popular manufacturing techniques that have been employed in fabricating filters include printed circuit board (PCB) [21], low temperature co-fired ceramic (LTCC) [22] and liquid crystal polymer (LCP) [23]. In terms of low cost and commercial availability, the PCB wins and hence, has been utilized in the fabrication of the BPF reported in this paper.
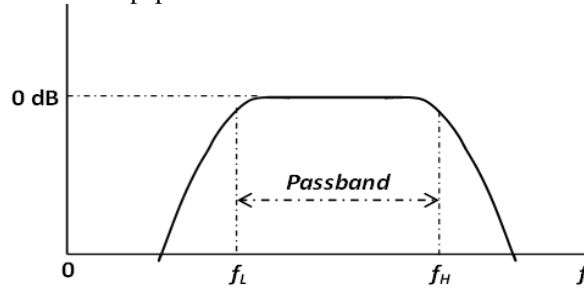
Figure 1. Channel/bandpass filter characteristics.

2.   FILTER CIRCUIT MODEL

The BPF circuit model was established from the standard normalized 3-pole Chebyshev lowpass prototype filter shown in Figure 2 [21], where g is the filter parameter. The proposed BPF is designed to have a center frequency, f_0 of 2.6 GHz, a fractional bandwidth of 3%, a passband ripple of 0.04321 dB, and a passband return loss of 20 dB.
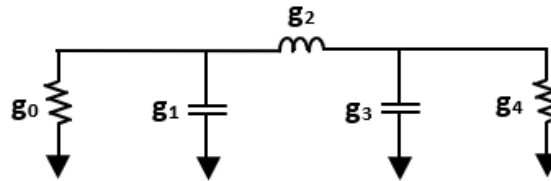
Figure 2. Standard normalized 3-pole/3rd order lowpass prototype filter ($g_0 = g_4 = 1.0$, $g_1 = g_3 = 0.8516$, $g_2 = 1.1032$).

The first step to designing the BPF circuit model is to transform the 3rd order lowpass prototype filter of Figure 2 into the BPF circuit shown in Figure 3. The transformation is based on Equations (1) and (2) [24], where Z_0 is the 50 Ohms characteristics impedance at the input and output terminations, *FBW* is the fractional bandwidth, ω_o is the angular center frequency of the BPF, C_s and L_s are the series capacitance and inductance respectively, while C_p and L_p are the parallel capacitance and inductance, respectively.

The second step of the BPF circuit model design is to use J-inverters to convert the series elements (i.e., C_s and L_s) in Figure 3 into shunt/parallel elements as shown in Figure 4. Hence, the BPF circuit model shown in Figure 4 contains only parallel *LC* elements, where $L = L_p$ and $C = C_p$. The numerical values for the J-inverters in Figure 4 were calculated using Equation (3) [24].
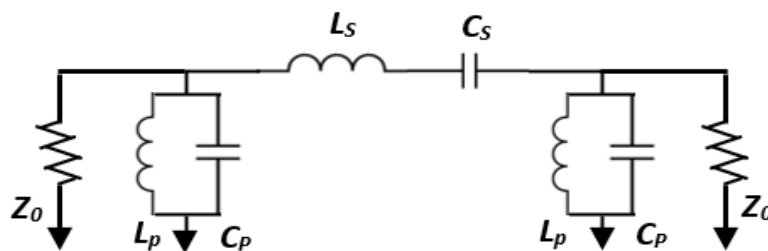
Figure 3. Bandpass filter circuit both series and parallel *LC* resonators ($C_p = 34.7529$ pF, $L_p = 0.1078$ nH, $C_s = 0.0333$ pF, $L_s = 112.551$ nH).

$$C_p = {g_1}/{\omega_0 Z_0 FBW} \; ; \qquad L_p = {Z_0 FBW}/{g_1 \omega_0} \qquad (1)$$

$$C_s = {FBW}/{g_2 \omega_0 Z_0} \; ; \qquad L_s = {g_2 Z_0}/{\omega_0 FBW} \qquad (2)$$

$$J_{01} = {g_0}/{Z_0} \; ; \qquad J_{12} = {\sqrt{{g_1^2}/{g_1 g_2}}}/{Z_0} \qquad (3)$$

$$C_J = {J}/{\omega_0} \qquad (4)$$
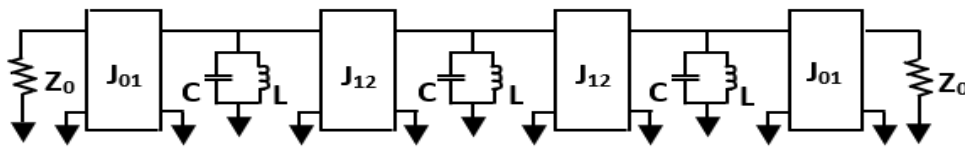
Figure 4. Bandpass filter circuit model with shunt/parallel-only identical *LC* resonators and J-inverters (*C* = C_p and *L* = L_p).

The third step of the BPF circuit model design is to replace each J-inverter in Figure 4 with a pi-network of capacitors or a pi-network of inductors as shown in Figure 5 [24]. Working with Figure 5 (b), the BPF circuit in Figure 4 is then transformed the final BPF circuit model shown in Figure 6 using Equation (4) [24]. This final circuit model is suitable for direct simulation in any commercially available computer-aided design (CAD) tool. Some examples of CAD tools that can be used for the simulation include the electronic design automation (EDA) circuit simulators listed in Table 1.

The fourth and final step is to simulate the BPF circuit model. The Keysight ADS circuit simulator was used in the circuit model simulation. The simulation results are shown in Figure 7. The results clearly show that the design targets were met as the center frequency is at 2.6 GHz as designed. The return loss is also better than 20 dB as expected. The insertion loss is at 0 dB as expected for an ideal (i.e., circuit model) filter.

(a)

(b)
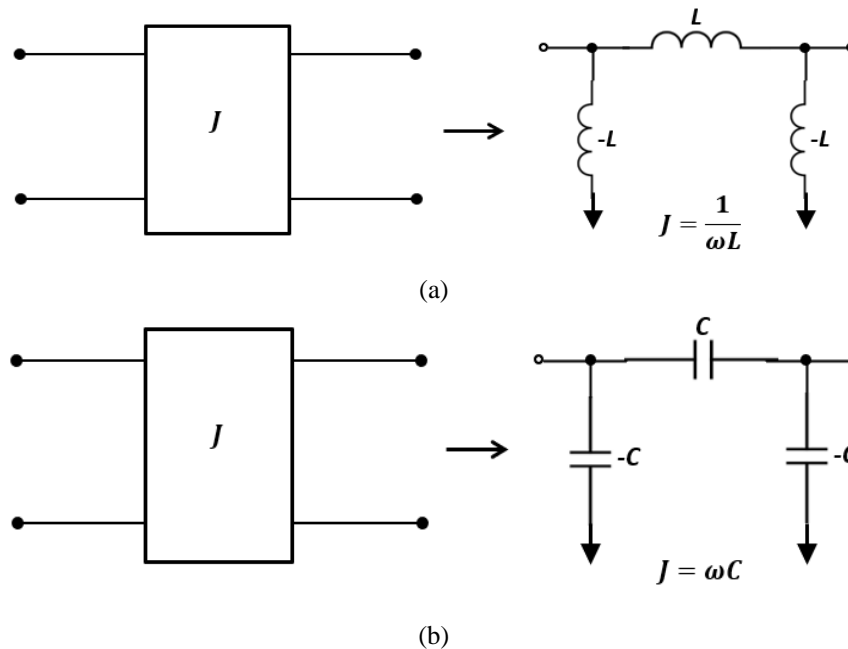
Figure 5. Reactive circuit elements modelling of admittance inverter: (a) J-inverter to pi-network of inductors; (b) J-inverter to pi-network of capacitors.

Table 1. Some commercially available electronic design automation tools

Company	Typical product	Type
Ansoft www.ansoft.com	HFSS	3D EM simulator
Applied Wave Research (AWR) www.awr.com	Microwave Office	Integrated package including linear and nonlinear circuit simulators, optimizers, and EM analysis tools
CST www.cst.com	CST Microwave Studio	3D EM simulator
EM Works www.emworks.com	HFWorks	3D EM simulator
Keysight Technologies www.keysight.com	Advanced Design System (ADS)	Integrated package including 3D EM simulators
	Electromagnetic Professional (EMPro)	3D EM simulator
	Genesys	Integrated EM simulation package
Sonnet Software www.sonnetsoftware.com	Sonnet Suites	3D planar EM software
	Sonnet Lite	Free 3D planar EM simulator
QWED www.qwed.com.pl	Quick Wave-3D	3D EM simulator
Zeland Software www.zeland.com	IE3D	Planar and 3D EM simulation, optimization, and synthesis package
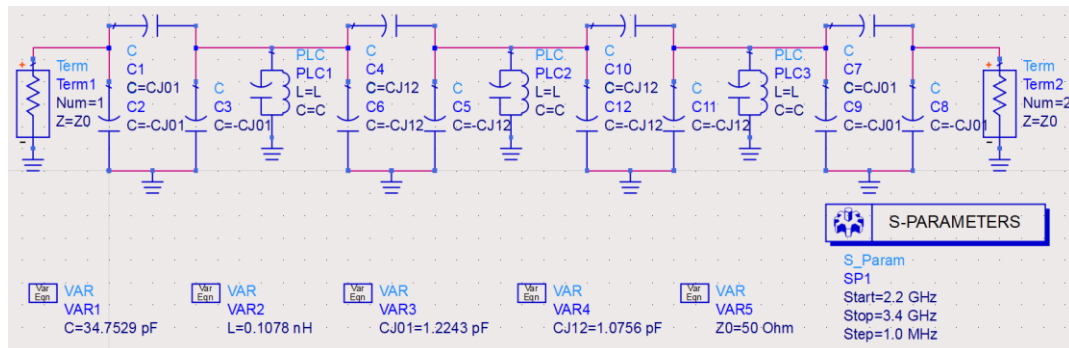
Figure 6. Bandpass filter circuit model in ADS circuit simulator, with shunt/parallel-only identical *LC* resonators and pi-network of capacitors replacing J-inverters.
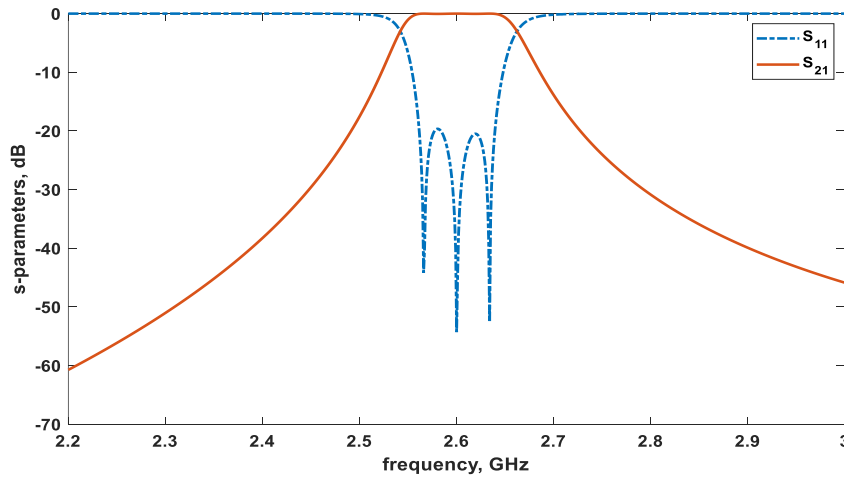
Figure 7. Simulation results of the bandpass filter circuit model.

3. MICROSTRIP LAYOUT IMPLEMENTATION

This section covers the microstrip implementation of the proposed channel filter using the microstrip hairpin resonator. This type of resonator is well-known for its simple structure, flexibility, and compact size. The resonator is achieved by folding the conventional half-wavelength resonator into a "U" shape. Hence, hairpin resonator filters are designed based on the same set of equations employed in the design of parallel-

coupled half-wavelength resonator filters [24]. When folding the half-wavelength resonator to achieve a hairpin resonator, it is important to consider the reduction of the coupled-line lengths, which reduces the coupling between resonators. Should the two arms of a hairpin be closely spaced, they will function as a pair of coupled lines, and this can also influence the coupling [24]. This section will be divided into subsections, with each subsection covering a step in the microstrip implementation of the BPF circuit model achieved in section 2.

3.1. Microstrip Hairpin Resonator Dimensions

The microstrip hairpin resonator (HPR) is designed to resonate at the proposed BPF center frequency, i.e., f_0. The design is made on Rogers RT/Duroid 6010LM substrate with a dielectric constant, ε_r, of 10.7, a thickness, h, of 1.27 mm and a loss tangent of 0.0023. The width (w) and length (l) of the microstrip were estimated from [24] using Equations (5) and (6), respectively. Note that ε_{eff} is the effective dielectric constant of the design material, c_0 (i.e., 3 x 10^8 m/s) is the speed of light in free space and $l = \lambda_g/2$, where λ_g is the guided wavelength. Using Equations (5) and (6), the design values for w and l were estimated to be 1.14 mm and 21.61 mm, respectively. The actual dimensions of the microstrip were achieved by using the estimated values on various rounds of simulation and optimization in ADS momentum. The actual dimensions were reached at the point where the microstrip HPR started resonating at f_o as shown in Figure 8.

$$w = \frac{8h\,e^A}{e^{2A}-2} \;; \quad A = \frac{Z_0}{60}\sqrt{\frac{\varepsilon_r+1}{2}} + \frac{\varepsilon_r-1}{\varepsilon_r+1}\left[0.23 + \frac{0.11}{\varepsilon_r}\right] \tag{5}$$

$$l = \frac{c_0}{2f_0\sqrt{\varepsilon_{eff}}} \;; \quad \varepsilon_{eff} = \frac{\varepsilon_r+1}{2} + \frac{\varepsilon_r-1}{2}\left(1 + 12\frac{h}{w}\right)^{-0.5} \tag{6}$$
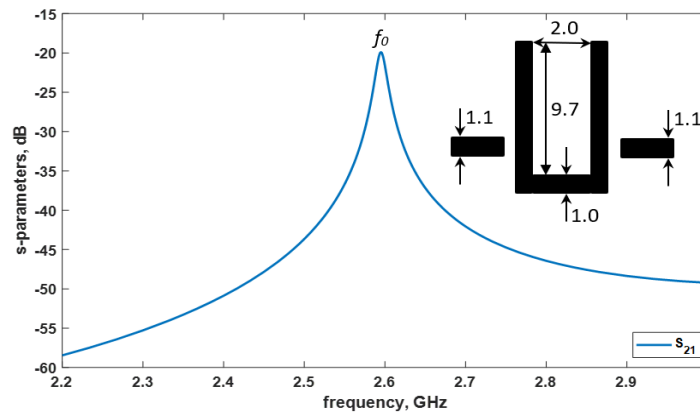
Figure 8. Hairpin resonator layout and response at 2.6 GHz (all dimensions in mm).

3.2. Coupling Coefficient Extraction

The coupling arrangement for the 3-pole channel filter is shown in Figure 9, where Q_{ext} is the external quality factor (to be discussed in the next subsection). The theoretical coupling between adjacent microstrip hairpin resonators is calculated to be 0.031 using Equation (7) [24], while the practical coupling value is achieved using Equation (8) [24] and the simulation technique shown in Figure 10. The separation distance, s, between adjacent resonators as shown in Figure 10, is the distance in mm that corresponds to the theoretical coupling value of 0.031, f_1 and f_2 are the eigen-modes from simulating the pair of coupled microstrip resonators. The matrix of k for the proposed bandpass filter is given in Equation (9).
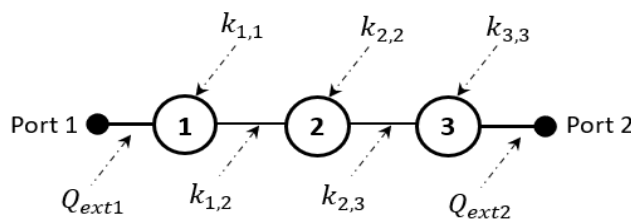
Figure 9. Coupling arrangement for the proposed 3-pole bandpass filter

$$\text{Theoretical coupling}: \quad k_{1,2} = k_{2,3} = \frac{FBW}{\sqrt{g_1 g_2}} \tag{7}$$

$$\text{Practical coupling}: \quad k = \frac{(f_2^2 - f_1^2)}{(f_2^2 + f_1^2)} \tag{8}$$

$$k = \begin{bmatrix} k_{1,1} & 0.031 & k_{1,3} \\ 0.031 & k_{2,2} & 0.031 \\ k_{3,1} & 0.031 & k_{3,3} \end{bmatrix} \tag{9}$$
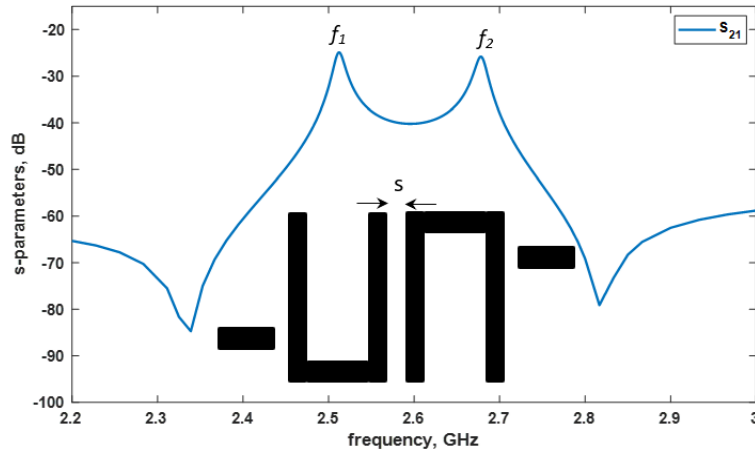
Figure 10. Coupling coefficient extraction technique for adjacent hairpin resonators (s = 1.9 mm).

3.3. External Quality Factor Extraction

The theoretical external quality factor value is calculated to be 28.387 using Equation (10). The practical value of the Q_{ext} is determined using Equation (11) and the technique shown in Figure 11. The separation distance, t, between the first (or the last) resonator and the input (or the output) port as shown in Figure 11, is the distance in mm that corresponds to the theoretical Q_{ext} value of 28.387. Hence, both Q_{ext1} and Q_{ext2} shown in Figure 9 are equal to 28.387.

$$\text{Theoretical } Q_{ext} = \frac{g_0 g_1}{FBW} \tag{10}$$

$$\text{Practical } Q_{ext} = \frac{f_0}{(f_2 - f_1)} \tag{11}$$
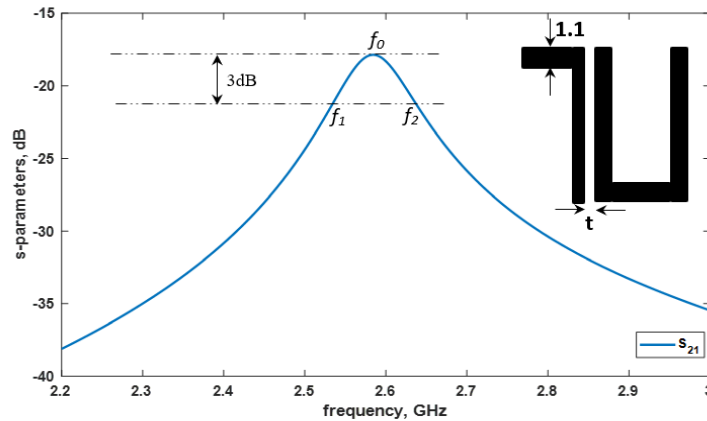
Figure 11. External quality factor extraction technique (t = 0.7, all dimensions in mm).

3.4. Filter Layout and Simulation

The proposed channel filter was put together based on the coupling arrangement of Figure 9. The filter layout was simulated using the Keysight ADS momentum full-wave electromagnetic simulator, with the layout

and simulation results shown in Figure 12. The simulation results are in good agreement with the circuit model results previously presented in Figure 7. However, unlike the circuit model design that is in ideal condition (i.e., lossless), the microstrip layout implementation of the BPF included both conductor and dielectric losses. The loss tangent of the dielectric materials was kept at 0.0023, while the copper conductivity used for the simulation was maintained at 5.8×10^7 S/m, with a thickness of 35 micron for both the top and bottom metals of the microstrip line. Surface roughness and thickness variation of the substrate material were not considered. As a result of the lossy simulation, a simulated minimum insertion loss of better than 1.8 dB was recorded, with a better than 25 dB minimum return loss. The simulation center frequency is at 2.6 GHz as designed.
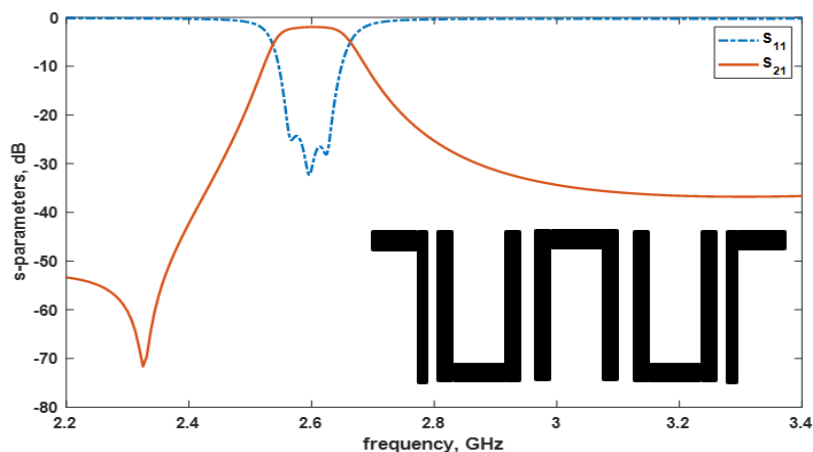
Figure 12. Layout and simulation results of the proposed 3-pole bandpass/channel filter.

4.   FABRICATION

The proposed BPF was fabricated using the same material employed in the electromagnetic simulation of the microstrip layout. Radio frequency printed circuit board (PCB) milling process technique was utilised for the circuit fabrication. A photograph of the fabricated microstrip BPF is shown in Figure 13. The overall size of the fabricated filter is 18.0 mm by 10.7 mm, i.e., $0.16\lambda g \times 0.09\lambda g$, where λg is the guided wavelength of the 50 Ω microstrip line at 2.6 GHz. A 50 Ohms SMA (sub-miniature version A) connector was attached to each port of the fabricated filter to facilitate measurement using Keysight Vector Network Analyzer.
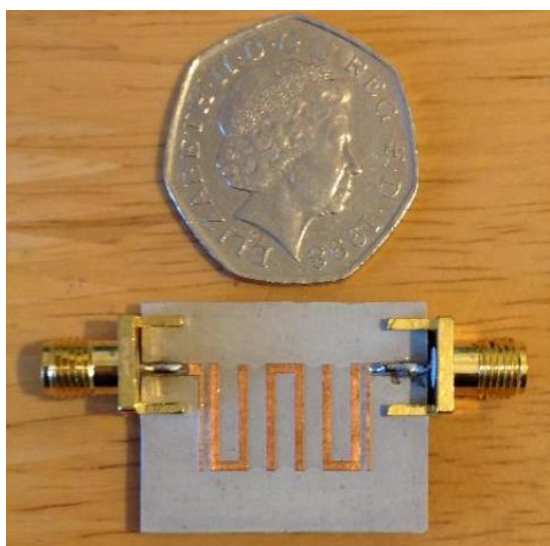
Figure 13. Photograph of the fabricated bandpass/channel filter.

5.   DISCUSSION

The circuit model and microstrip layout results of the proposed BPF are co-presented in Figure 14 for easy comparison. The solid lines in Figure 14 represent the circuit model results while the dashed lines

represent the microstrip layout simulation results of the filter. The proposed filter performance was compared with some related published works using Table 2. The comparison with [17, 20, 25] clearly shows that the proposed BPF is of compact size, with a good insertion loss. The minimum return loss is excellent at 25 dB.
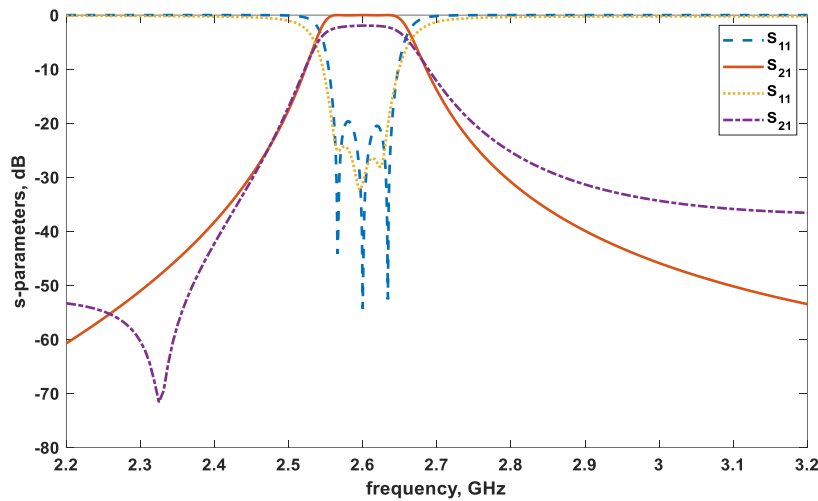
Figure 14. Comparison of the circuit model and the microstrip layout results of the proposed BPF.

Table 2. Comparison of the proposed filter performances with related published works.

Ref.	f_0 (GHz)	Filter Order	Size (λ_g x λ_g)	IL[1] (dB)	RL[2] (dB)
[17]	4.50	2	0.28 x 0.09	1.6	10.0
[20]	3.35	2	0.12 x 0.09	2.4	20.0
[25]	2.45	2	0.15 x 0.13	2.4	20.0
This work	2.60	3	0.16 x 0.09	1.8	25.0

[1] insertion loss, [2] return loss.

6.   CONCLUSIONS

A 3rd order (3-pole) bandpass filter has been proposed, designed, and implemented using the microstrip transmission line technology. The design was completely based on well-known formulations and relied on microstrip hairpin resonators for miniaturisation. The circuit model and microstrip layout results show good agreement; with centre frequency of 2.6 GHz, good selectivity and sharp roll-off. The simulation measured minimum insertion loss of less than 1.8 dB, and minimum in-band return loss of greater than 25 dB were achieved. The fabricated filter is of compact size with a small footprint of 18.0 mm by 10.7 mm (i.e., 0.16λg x 0.09λg), where λg is the guided wavelength of the 50 Ω microstrip line at the center frequency of the bandpass filter.

REFERENCES

[1]   Nwajana, A.O.; Dainkeh, A.; Yeo, K.S.K. Substrate integrated waveguide (SIW) bandpass filter with novel microstrip-CPW-SIW input coupling. *Journal of Microwaves, Optoelectronics and Electromagnetic Applications* **2017**, *16(2)*, pp. 393–402.

[2]   Liu, Y.-T.; Leung, K.W.; Yang, N. Compact absorptive patch antenna. *IEEE Transaction on Antennas and Propagation* **2020**, *68(2)*, pp. 633–642.

[3]   Wei, F.; Zhao, X.-B.; Shi, X.W. A balanced filtering quasi-Yagi antenna with low cross-polarization levels and high common-mode suppression. *IEEE Access* **2019**, 7, pp. 100113–100119.

[4]   Nwajana, A.O. Dual-band microwave filter for WiMax application, 1st ed.; Lambert Academic Publishing, Riga, Latvia, 2020; pp. 1–112.

[5]   Yeo, K.S.K.; Nwajana, A.O. A novel microstrip dual-band bandpass filter using dual-mode square patch resonators. *Progress In Electromagnetic Research C* **2013**, 36, pp. 233–247.

[6] Hou, Z.; Liu, C.; Zhang, B.; Song, R.; Wu, Z.; Zhang, J.; He, D. Dual-/tri-wideband bandpass filter wit high selectivity and adjustable passband for 5G mid-band mobile communications. *MDPI Electronics* **2020**, 9, 205.

[7] Nwajana, A.O.; Otuka, R.I.; Ebenuwa, S.H.; Ihianle, I.K.; Aneke, S.O.; Edoh, A.A. Symmetric 3dB filtering power divider with equal output power ratio for communication systems. Proceedings of the 2nd International Conference on Electrical, Communication and Computer Engineering (ICECCE), Istanbul, Turkey, June 2020; IEEE, pp. 1–4.

[8] Dainkeh, A.; Nwajana, A.O.; Yeo, K.S.K. Filtered power splitter using microstrip square open loop resonators. *Progress In Electromagnetic Research C* **2016**, 64, pp. 133–140.

[9] Nwajana, A.O.; Yeo, K.S.K. Multi-coupled resonator microwave diplexer with high isolation. Proceedings of the 46th European Microwave Conference (EuMC), London, UK, October 2016; IEEE, pp. 1167–1170.

[10] Nwajana, A.O.; Dainkeh, A.; Yeo, K.S.K. Substrate integrated waveguide (SIW) diplexer with novel input/output coupling and no separate junction. *Progress In Electromagnetic Research M* **2018**, 67, pp. 75–84.

[11] Shi, Y.; Zhang, J.; Zhou, M.; Feng, W.; Cao, B.; Che, W. Miniaturized W-band gap waveguide bandpass filter using the MEMS technique for both waveguide and surface mounted packaging. *IEEE Transactions on Circuits and Systems–II: Express Briefs* **2019**, 66(6), pp. 938–942.

[12] Dahle, R.; Laforge, P.; Kuhling, J. 3-D printed customizable inserts for waveguide filter design at X-band. *IEEE Microwave and Wireless Components Letters* **2017**, 27(12), pp. 1080–1082.

[13] AbuHussain, M.; Hasar, U.C. Design of X-bandpass waveguide Chebyshev filter based on CSRR metamaterial for telecommunication systems. *MDPI Electronics* **2020**, 9, 101.

[14] Huang, F.; Wang, J.; Zhu, L. A new approach to design a microstrip dual-mode balun bandpass filter. *IEEE Microwave and Wireless Components Letters* **2016**, 26(4), pp. 252–254.

[15] Nwajana, A.O.; Yeo, K.S.K. Microwave diplexer purely based on direct synchronous and asynchronous coupling. *Radioengineering* **2016**, 25(2), pp. 247–252.

[16] Cai, C.; Wang, J.; Zhu, L.; Wu, W. A new approach to design a microstrip wideband balun bandpass filter. *IEEE Microwave and Wireless Components Letters* **2016**, 26(2), pp. 116–118.

[17] Zhang, P.; Liu, L.; Chen, D.; Weng, M.-H.; Yang, R.-Y. Application of a stub-loaded square ring resonator for wideband bandpass filter design. *MDPI Electronics* **2020**, 9, 176.

[18] Qui, L.-F.; Wu, L.-S.; Xie, B.; Yin, W.-Y.; Mao, J.-F. Substrate integrated waveguide filter with flat passband based on complex couplings. *IEEE Microwave and Wireless Components Letters* **2018**, 28(6), pp. 494–496.

[19] Azad, A.R.; Mohan, A. Substrate integrated waveguide dual-band and wide-stopband bandpass filters. *IEEE Microwave and Wireless Components Letters* **2018**, 28(8), pp. 660–662.

[20] Hu, S.; Hu, Y.; Zheng, H.; Zhu, W.; Gao, Y.; Zhang, X. A compact 3.3–3.5 GHz filter based on modified composite right–/left–handed resonator units. *MDPI Electronics* **2020**, 9, 1.

[21] Nwajana, A.O.; Yeo, K.S.K.; Dainkeh, A. Low cost SIW Chebyshev bandpass filter with new input/output connection. Proceedings of the 16th Mediterranean Microwave Symposium (MMS), Abu Dhabi, UAE, November 2016; IEEE, pp. 1–4.

[22] Wong, S.-W.; Wang, K.; Chen, Z.-N.; Chu, X.-Q. Electric coupling structure of substrate integrated waveguide (SIW) for the application of 140-GHz bandpass filter on LTCC. *IEEE Transactions on Components, Packaging and Manufacturing Technology* **2014**, 4(2), pp. 316–322.

[23] Dalmia, S.; White, G.; Sundaram, V.; Swaminathan, M. Design of quasi-lumped element diplexer for multiple wireless applications using liquid crystalline polymer (LCP) based substrates. Proceedings of the 34th European Microwave Conference (EuMC), Amsterdam, The Netherlands, October 2004; IEEE, pp. 737–740.

[24] Hong, J.-S. Microstrip filters for RF/microwave applications, 2nd ed.; Wiley, New York, USA, 2011; pp. 1–635.

[25] Jung, E.-Y.; Hwang, H.-Y. A balun-BPF using a dual-mode ring resonator. *IEEE Microwave and Wireless Components Letters* **2007**, 17(9), pp. 652–654.

BIOGRAPHY OF AUTHOR

Augustine O. Nwajana received the PhD in Electrical and Electronic Engineering from the University of East London, UK, in 2017 and a research CPD certificate in Practical Antenna Design: from Theory to Practice, from the University of Oxford, UK, in 2019. From 2005 to 2009, he was a Telecommunications Engineer with Siemens AG where his experience spanned many countries including the USA, UK, UAE, Germany, South Africa, Ghana, and Nigeria. He was also with Coventry University (as an associate lecturer) and with the University of East London (as a part-time lecturer).

Dr. Nwajana is currently a lecturer with the University of Greenwich. His current research interest is in the analysis and design of RF and microwave devices (including SIW and microstrip filters, diplexers/multiplexers, power dividers/combiners, couplers, antennas, etc.) for modern communication systems. He has authored/co-authored five books, ten articles, and five conference papers. He is currently serving as Editor for IGI Global USA and Guest Editor for MDPI Switzerland. He is also a Senior Member of the Institute of Electrical and Electronics Engineers (SMIEEE), and a Fellow of the UK Higher Education Academy (FHEA). He was a recipient of the Federal Government of Nigeria Scholarship Award.